Gastroenterology 2014;147:1119–1133

Nicotine Promotes Initiation and Progression of KRAS-Induced Pancreatic Cancer via *Gata6*-Dependent Dedifferentiation of Acinar Cells in Mice

Patrick C. Hermann,[1,*] Patricia Sancho,[1,*] Marta Cañamero,[2] Paola Martinelli,[3] Francesc Madriles,[3] Patrick Michl,[4] Thomas Gress,[4] Ricardo de Pascual,[5] Luis Gandia,[5] Carmen Guerra,[6] Mariano Barbacid,[6] Martin Wagner,[7] Catarina R. Vieira,[1] Alexandra Aicher,[1] Francisco X. Real,[3] Bruno Sainz Jr,[1] and Christopher Heeschen[1,8]

[1]*Stem Cells and Cancer Group,* [2]*Comparative Pathology Core Unit,* [3]*Epithelial Carcinogenesis Group, Spanish National Cancer Research Centre (CNIO), Madrid, Spain;* [4]*Department of Gastroenterology, Endocrinology, Metabolism and Infectiology, University of Marburg, Marburg, Germany;* [5]*Instituto Teófilo Hernando, Facultad de Medicina, Universidad Autónoma de Madrid, Madrid, Spain;* [6]*Experimental Oncology Group, Spanish National Cancer Research Centre (CNIO), Madrid, Spain;* [7]*Department of Internal Medicine I, Ulm University, Ulm, Germany; and* [8]*Centre for Stem Cells in Cancer & Ageing, Barts Cancer Institute, Queen Mary University of London, UK*

See Covering the Cover synopsis on page 947; see editorial on page 962.

BACKGROUND & AIMS: Although smoking is a leading risk factor for pancreatic ductal adenocarcinoma (PDAC), little is known about the mechanisms by which smoking promotes initiation or progression of PDAC. **METHODS:** We studied the effects of nicotine administration on pancreatic cancer development in *Kras*$^{+/LSLG12Vgeo}$*;Elas-tTA/tetO-Cre* (Ela-KRAS) mice, *Kras*$^{+/LSLG12D}$*;Trp53+/LSLR172H;Pdx-1-Cre* (KPC) mice (which express constitutively active forms of KRAS), and C57/B6 mice. Mice were given nicotine for up to 86 weeks to produce blood levels comparable with those of intermediate smokers. Pancreatic tissues were collected and analyzed by immunohistochemistry and reverse transcriptase polymerase chain reaction; cells were isolated and assayed for colony and sphere formation and gene expression. The effects of nicotine were also evaluated in primary pancreatic acinar cells isolated from wild-type, *nAChR7a*$^{-/-}$, *Trp53*$^{-/-}$, and Gata6$^{-/-}$*;Trp53*$^{-/-}$ mice. We also analyzed primary PDAC cells that overexpressed GATA6 from lentiviral expression vectors. **RESULTS:** Administration of nicotine accelerated transformation of pancreatic cells and tumor formation in Ela-KRAS and KPC mice. Nicotine induced dedifferentiation of acinar cells by activating AKT–ERK–MYC signaling; this led to inhibition of *Gata6* promoter activity, loss of GATA6 protein, and subsequent loss of acinar differentiation and hyperactivation of oncogenic KRAS. Nicotine also promoted aggressiveness of established tumors as well as the epithelial–mesenchymal transition, increasing numbers of circulating cancer cells and their dissemination to the liver, compared with mice not exposed to nicotine. Nicotine induced pancreatic cells to acquire gene expression patterns and functional characteristics of cancer stem cells. These effects were markedly attenuated in *K-Ras*$^{+/LSL-G12D}$*;Trp53*$^{+/LSLR172H}$*; Pdx-1-Cre* mice given metformin. Metformin prevented nicotine-induced pancreatic carcinogenesis and tumor growth by up-regulating GATA6 and promoting differentiation toward an acinar cell program. **CONCLUSIONS:** In mice, nicotine promotes pancreatic carcinogenesis and tumor development via down-regulation of *Gata6* to induce acinar cell dedifferentiation.

Keywords: Progenitor Cells; Metastasis; Pancreas; Mouse Model.

In patients with pancreatic ductal adenocarcinoma (PDAC), one fourth of deaths are linked to tobacco use, and heavy smoking is associated with a 6-fold increased risk of developing PDAC.[1] Although the number of smoking-related mutations in the pancreas is not as high as in lung cancer, smokers with PDAC harbor more mutations than nonsmokers, but the increased mutation frequencies are generally not found in PDAC "driver" genes.[2] Therefore, although smokers may develop PDAC more frequently and earlier, driver mutations appear to remain the same, suggesting the involvement of other mechanisms promoting pancreatic carcinogenesis in smokers.

Among the thousands of substances in cigarette smoke, nicotine has been studied extensively because of its addictive properties. Although not carcinogenic,[3] nicotine may still be implicated in the initiation and progression of PDAC via nicotinic acetylcholine receptor (nAChR)-mediated modulation of cell functions. Recent discoveries show that nAChRs modulate proliferation and apoptosis of cancer cells in the pancreas.[4] Although stimulatory effects of nicotine on established cancer cell lines have been convincingly demonstrated,[4,5] the consequences of nicotine on *K-*

*Authors share co-first authorship.

Abbreviations used in this paper: **AMPK, adenosine monophosphate–activated protein kinase; CSC, cancer stem cell; EMT, epithelial-mesenchymal transition; ERK, extracellular signal–regulated kinase; KPC, *Kras*$^{+/LSLG12D}$*;Trp53+/LSLR172H;Pdx-1-Cre*; nAChR, nicotinic acetylcholine receptor; PanIN, pancreatic intraepithelial neoplasia; PCR, polymerase chain reaction; PDAC, pancreatic ductal adenocarcinoma; ROS, reactive oxygen species; wt, wild-type.**

0016-5085/$36.00
http://dx.doi.org/10.1053/j.gastro.2014.08.002

Ras–initiated PDAC development have not been rigorously investigated to date.

The crucial initiating step for PDAC development has been associated with near-universal activating mutations in the *K-Ras* gene[6,7]; however, such mutations are not biomarkers for disease because they can be frequently detected in healthy individuals,[8] and mutant *K-Ras* alone is not oncogenic in adult mice.[7] The incidence of *K-Ras* mutations in the pancreas increases with age, and median PDAC diagnosis age is 15 years earlier in smokers (56 years) vs nonsmokers (71 years) in hereditary pancreatitis.[9] Depending on the context, several cell types may act as the "cell-of-origin," ranging from differentiated cells to multipotent stem cells, but concomitant tissue alterations are required for progression to PDAC[7], and nicotine may accelerate this transformation process in *K-Ras* mutant cells.

Materials and Methods

Mice

The *K-Ras*$^{+/LSLG12Vgeo}$;*Elas*-tTA/tetO-Cre Ela-KRAS and *K-Ras*$^{+/LSL-G12D}$;*Trp53*$^{LSL-R172H}$;*Pdx-1*-Cre (KPC) mouse models of pancreatic cancer have been described previously.[7,10] B6.129S7-*Chrna7*^{tm1Bay}/J mice were obtained from Jackson Laboratories (Bar Harbor, ME). Mice were screened for PDAC using a small animal ultrasound system (Visualsonics, Toronto, Ontario). Mice were housed according to institutional guidelines; all experiments were approved by the ISCIII Ethical Committee and performed in accordance with the guidelines for Ethical Conduct in the Care and Use of Animals as stated in The International Guiding Principles for Biomedical Research involving Animals, developed by the CIOMS.

Cells

Pancreatic tumors from Ela-KRAS mice (AAU77G) and KPC mice (CHX6, CHX45) were cut into pieces, enzymatically digested with collagenase and cultured as described previously.[11] Epithelial clones were pooled and further expanded to heterogeneous primary murine PDAC cell lines. Murine wild-type and *Gata6*$^{-/-}$ pancreatic acinar cells were isolated from *Ptf1a*^{Cre};R26R-LSL-EYFP; *Trp53*$^{-/-}$ and *Gata6*$^{loxP/loxP}$; *Ptf1a*^{Cre}; R26R-LSL-EYFP; *Trp53*$^{-/-}$ mice, respectively, as described previously.[7,11,12] *Kras*^{G12V}-Caerulean pancreatic acinar cells or *Gata6*-GFP-expressing murine PDAC cells were established by infecting cells with respective lentiviral vectors. Firefly luciferase expressing PDAC cells were established by infecting cells with the CMV-Luciferase-RFP-TK Lentivector system from BioCat GmbH (Heidelberg, Germany). Transduced cells were subsequently sorted for Caerulean (FACS ARIA IIu; BD), red fluorescent protein and/or green fluorescent protein (InFlux; Cytopeia-BD) and further expanded.

Additional methods can be found in the Supplementary Materials.

Results

Nicotine Promotes K-Ras–Induced Carcinogenesis

To study the effects of nicotine on early pancreatic carcinogenesis, we used *K-Ras*$^{+/LSLG12Vgeo}$;*Elas*-tTA/tetO-Cre (Ela-KRAS) mice[7] with constitutively active *K-Ras*^{G12V}. Mice were treated with nicotine for 86 weeks (Supplementary Figure 1*A*), resulting in cotinine levels comparable with intermediate smokers (Supplementary Figure 1*B*, *left*)[13] and no significant changes in body weight (Supplementary Figure 1*B*, *right*). We did, however, observe severe morphologic changes in the pancreata (Figure 1*A*). Both the area of pancreatic intraepithelial neoplasia (PanIN) lesions (Figure 1*A*, *left*) and of acinar-to-ductal metaplasia + atrophy (Figure 1*A*, *right*) were significantly increased in nicotine-treated mice compared with control mice. We observed significantly more low-grade lesions and, more importantly, we observed high-grade (PanIN 2 and 3) lesions only in nicotine-treated mice (Figure 1*B*). In addition, we found increased proliferative activity of ductal cells within PanINs (Figure 1*C* and Supplementary Figure 1*E*). Importantly, we reproduced and expanded our findings in the more aggressive KPC mouse model of PDAC[10] (Figures 1*D*–*E* and Supplementary Figure 1*F*). Lastly, and in accordance with the observation that nicotine itself is not carcinogenic,[3] we observed no neoplastic lesions in nicotine-treated C57/B6 wild-type (wt) mice. These mice neither displayed evidence of pancreatitis (Supplementary Figure 1*C*), nor showed significant tissue damage by histology (Supplementary Figure 1*D*).

We also observed striking alterations within the stromal compartment, including increased macrophage infiltration (Supplementary Figure 1*F*, *left*; Supplementary Figure 1*G*), notably an increase in strongly YM-1–positive lesions in the nicotine group, suggesting an additional pro-tumorigenic effect mediated by M2-polarized macrophages (Figure 1*F*, *right* and Supplementary Figure 1*H*). Importantly, virtually no macrophage infiltration was observed in long-term–treated C57/B6 wt mice (Supplementary Figure 1*D*, *right*), ruling out acute or chronic pancreatitis as the initiating event, and demonstrating that the increased inflammatory/stromal cells were secondary, rather than causative.

Nicotine Modulates the Transcriptional Program of the Acinar Compartment

Gata6 and *Mist1* are key regulators of acinar cell differentiation,[14,15] and loss of acinar differentiation has been linked to increased metaplasia.[16] As this may represent the initial step of *K-Ras*–driven tumorigenesis,[7,17] we first investigated the expression of these regulators in nicotine-treated C57/B6 mice to exclude effects of *K-Ras* mutations and inflammation. *Gata6* and *Mist1* mRNA levels were downregulated 2 weeks post nicotine treatment (Figure 2*A*, *left*), and the differences were more striking after 86 weeks of treatment, and even detectable by immunohistochemistry (Figure 2*A*, *right*). Concomitantly, we also observed a strong decrease in mRNA levels of acinar genes, a strong reduction in acinar granularity, and reduced enzyme production, indicating a severe loss of acinar differentiation and enzyme production (Figure 2*B* and Supplementary Figure 2*A*), but with little tissue alterations observed by transmission electron microscopy (Supplementary Figure 2*B*). We also observed a significant increase in the number of proliferating

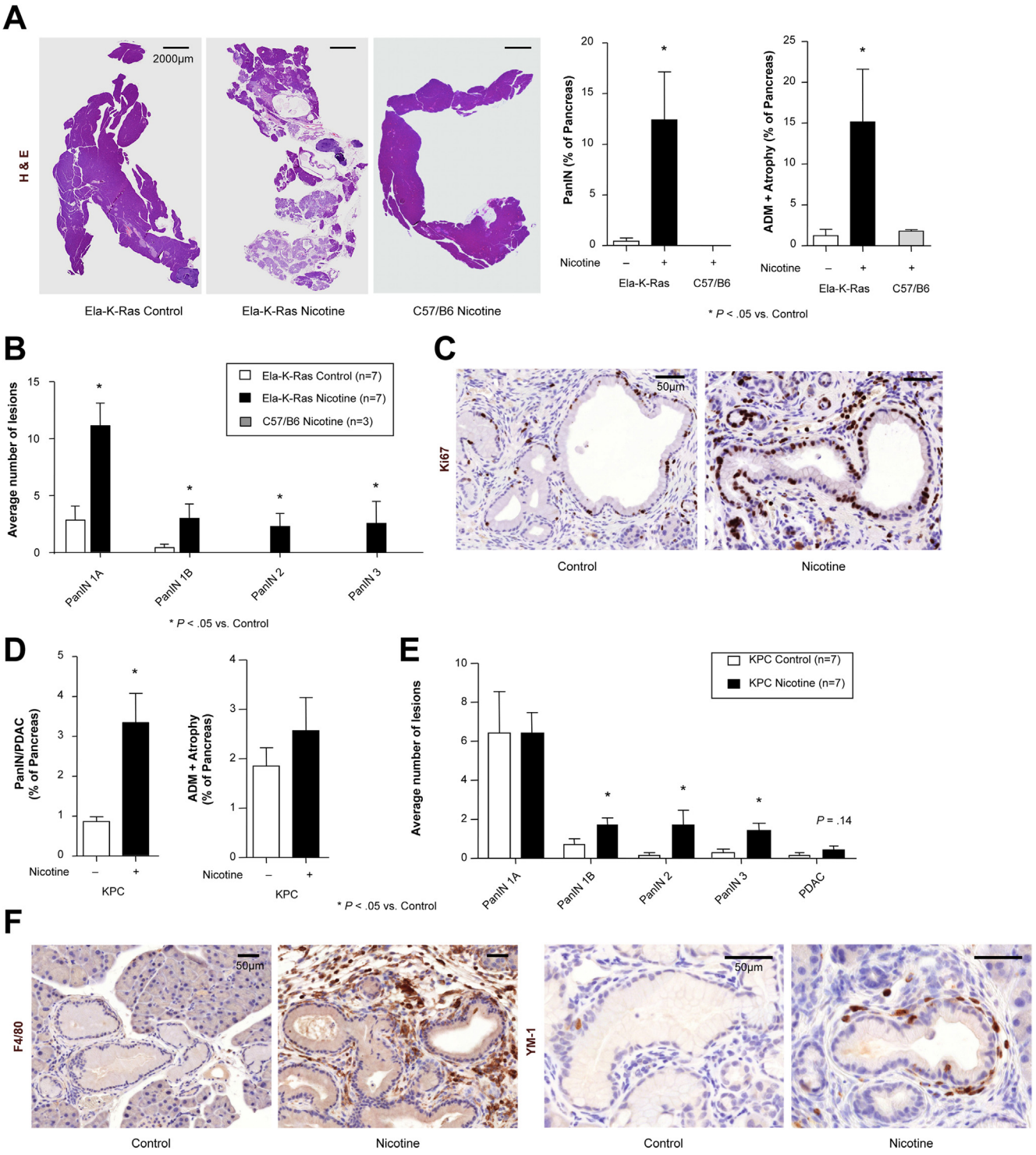

Figure 1. Nicotine promotes K-Ras–driven pancreatic carcinogenesis. (*A*) Representative images of mouse pancreata from control (n = 7) vs nicotine-treated (n = 7) Ela-KRAS and C57/B6 (n = 3) mice after 86 weeks of treatment. Quantification of tissue area damaged by PanIN (*left*) or acinar-to-ductal metaplasia (ADM) and atrophy combined (*right*). (*B*) Quantitative analysis of PanIN frequency and grading. (*C*) Representative images of Ki67 staining within PanIN lesions (semi-quantitative analysis of lesions is provided in Supplementary Figure 1*E*). (*D*) Quantification of tissue area damaged by PanIN (*left*) or ADM and atrophy combined (*right*) in control (n = 7) vs nicotine-treated (n = 7) KPC mice after 8 weeks of treatment. (*E*) Quantitative analysis of PanIN/PDAC frequency and grading. (*F*) Representative images of macrophage F4/80 marker staining (*left*) (semi-quantitative analysis of lesions is provided as Supplementary Figure 1*G*) and representative images of macrophage YM-1 M2 marker staining (*right*) (semi-quantitative analysis of lesions is provided as Supplementary Figure 1*H*).

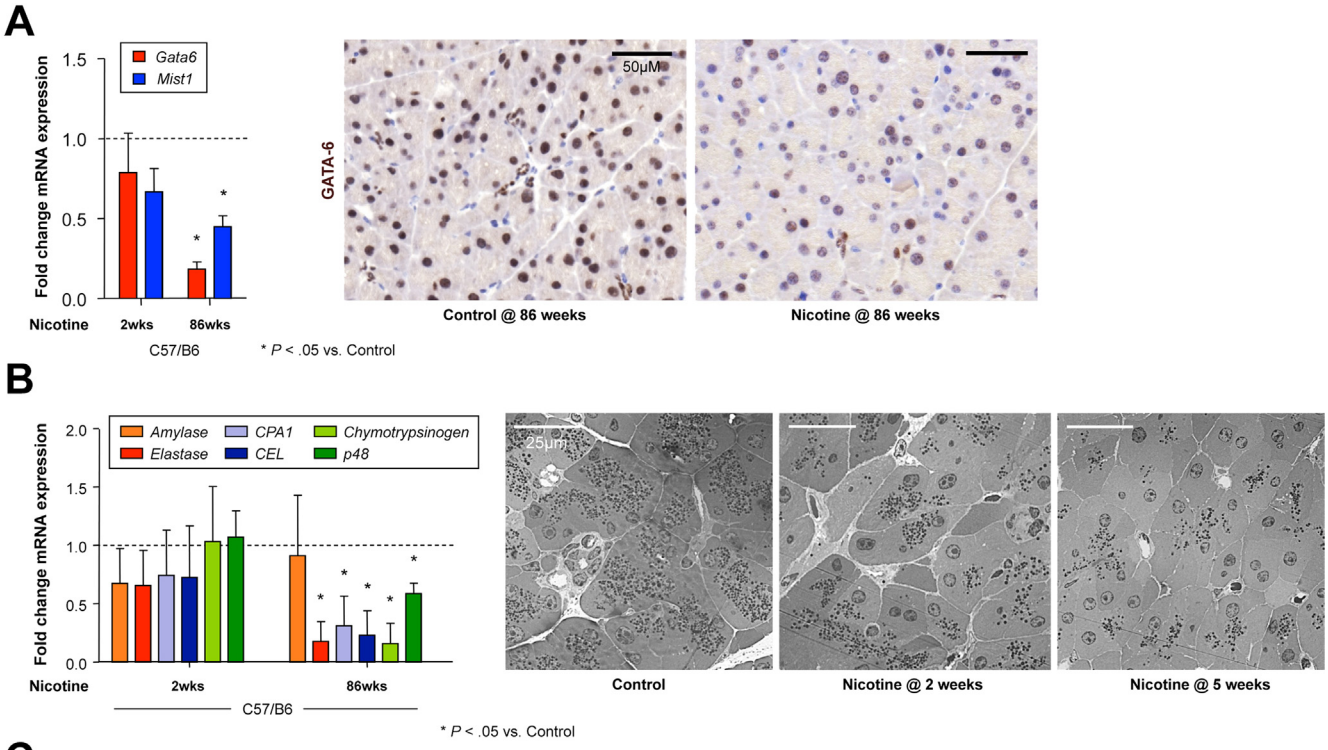
A
Gata6
Mist1
Fold change mRNA expression
1.5
1.0
0.5
0.0
Nicotine
2wks
86wks
C57/B6
* P < .05 vs. Control
GATA-6
50μM
Control @ 86 weeks
Nicotine @ 86 weeks
B
Amylase
Elastase
CPA1
CEL
Chymotrypsinogen
p48
Fold change mRNA expression
2.0
1.5
1.0
0.5
0.0
Nicotine
2wks
86wks
C57/B6
* P < .05 vs. Control
25μm
Control
Nicotine @ 2 weeks
Nicotine @ 5 weeks
C
Ki67+ cells
(% of all acinar cells)
2.0
1.5
1.0
0.5
0.0
Nicotine
–
+
C57/B6
Ki67
50μm
Control
Nicotine
D
Fold-change in Sox9 mRNA
60
40
20
4
3
2
1
0
Nicotine
2wks
86wks
C57/B6
* P < .05 vs. Control
E
Area of SOX9+ non-ductal cells
(% area of all cells)
4
3
2
1
0
Nicotine
–
+
KPC
50μm
50μm
20μm
Control
Nicotine
F
PSC
100 μm
Colony forming units
1/30,000 cells
100
75
50
25
0
Nicotine
–
+
–
+
Wild type
Ela-K-Ras
Colony forming units
(out of 3x10⁴ cells)
150
100
50
0
n.s.
Nicotine
–
+
–
+
Wild type
α7-nAChR-/-
* P < .05 vs. Control

acinar cells (Figure 2*C*), cells expressing aldehyde dehydrogenase (ALDH), a pancreatic progenitor marker[18] (Supplementary Figure 2*D*), and a marked up-regulation of the stemness-associated gene *Sox9* after nicotine treatment (Figure 2*D*). In addition, 8 weeks of nicotine treatment of KPC mice significantly increased the numbers of nonductal SOX9$^+$ cells in normal tissue, which reportedly represent progenitors capable of giving rise to ductal and acinar lineages[19] (Figure 2*E*). Of note, ectopic SOX9 expression in acinar cells leads to the development of pre-neoplastic lesions, a necessary step for *K-Ras*–induced malignant transformation.[19]

To provide functional evidence for enhanced acinar progenitor activity, we assessed the colony formation capacity of pancreas-derived cells. Intriguingly, pancreata of nicotine-treated C57/B6 and Ela-KRAS mice had significantly more colony-forming activity, and these colonies expressed higher levels of acinar and stemness genes (Figure 2 and Supplementary Figure 2*E*). Because the effects of nicotine are mediated via homomeric CNS-type α*7-nAChRs* (Supplementary Figure 2*F–G*) and subsequent Ca^{2+} influx,[20] we used B6.129S7-*Chrna7*^{tm1Bay}/J mice lacking α7-nAChR expression to demonstrate that the aforementioned effects with nicotine were specifically mediated via α*7-nAChR* (Figure 2*F, right*).

Nicotine Suppresses Gata6 *via Extracellular Signal–Regulated Kinase/MYC Pathway*

Having observed such a profound effect on acinar differentiation (eg, *Gata6* down-regulation), we set out to more rigorously dissect this phenotype. Using a *Gata6* promoter construct, we show that nicotine represses *Gata6* promoter activity in a concentration- and time-dependent manner in primary acinar cells (Figure 3*A, left*). In silico analysis identified 6 putative C-MYC binding sites within 9 kb of the transcriptional start site, suggesting C-MYC as a potential candidate for *Gata6* (promoter) binding (Figure 3*A, right*). In addition, a direct interaction between GATA6 and MYC has also been described and validated previously.[21] Along these lines, treatment of primary acinar cells with nicotine resulted in a marked increase in phospho-C-MYC and a concomitant repression of *Gata6* promoter activity, both of which could be reversed by silencing or pharmacologically inhibiting C-MYC (Figure 3*B*). We next measured 2 of the many signaling pathways upstream of MYC to better map the cascade of cellular events involved in nicotine-mediated repression of *Gata6*. We observed a time-dependent phosphorylation of AKT and extracellular signal–regulated kinase (ERK), and subsequently of C-MYC, by nicotine in primary murine acinar cells (Figure 3*C*, *left* and Supplementary Figure 3*A*), which we subsequently show are necessary for nicotine-mediated *Gata6* promoter repression as inhibitors of these pathways reversed this effect (Figure 3*C*, *middle*), likely via abrogating phospho-C-MYC's inhibitory effect on the *Gata6* promoter (Figure 3*C*, *right*).

Because *K-Ras* mutations are driving factors for PDAC development, we next studied the effects of nicotine in primary murine acinar cells overexpressing mutant *K-Ras*^{G12V}. As would be expected, independent of nicotine treatment, activation of ERK and C-MYC was noticeably greater in *K-Ras*^{G12V} mutant cells; however, the phosphorylation of these 2 proteins was unexpectedly increased further in the absence of *Gata6* (Figure 3*D*). Interestingly, both the loss of *Gata6* and the expression of mutant *K-Ras* were necessary to hyperactivate ERK as murine acinar cells lacking *Gata6* alone did not show a similar increased activation (Figure 3*C*). In line with these results, we also observed that nicotine hyperactivated RAS, but only in the context of *K-Ras*^{G12V} and *Gata6* loss (Figure 3*E*, *left*) and these results were confirmed in *K-Ras*^{wt} and *K-Ras*^{G12D} human PDAC cells (Figure 3*E*, *middle*).

Consistent with these findings, we also observed that although nicotine increased murine acinar cell proliferation similar to what we observed in vivo (Figure 2*C*), the effect was significantly enhanced in the absence of *Gata6* and in the presence of mutant *K-Ras*^{G12V} (Figure 3*E, right*). Importantly, this preferential effect was also observed in vivo. Although *K-Ras* wt cells were nontumorigenic, *K-Ras*^{G12V}-expressing cells reproducibly formed large tumors (Figure 3*F*), and nicotine treatment could further increase tumor burden, but only in *Gata6*-deficient cells. Therefore, the sum of these data indicate that the ultimate loss of *Gata6* creates a cellular environment favoring nicotine-mediated activation of mutant *K-Ras* and downstream K-RAS targets, such as ERK (Supplementary Figure 3*B*), promoting cellular proliferation and ultimately tumor growth.

Nicotine Promotes a Cancer Stem Cell Phenotype That Can Be Reversed by Gata6 *Overexpression*

In addition to promoting cellular plasticity during tumor initiation and early progression, we observed a strong

Figure 2. Nicotine modulates the transcriptional program of the acinar compartment. (*A*) Fold change in pancreas messenger RNA (mRNA) levels for the key acinar regulators *Gata6* and *Mist1* compared with control levels (*dotted line*) after 2 and 86 weeks of nicotine treatment, and nuclear GATA6 immunohistochemistry analysis after 86 weeks of nicotine treatment (n = 4). (*B*) Fold change in pancreas mRNA levels of acinar genes after 2 or 86 weeks of nicotine treatment compared with control levels (*dotted line*) (*left*) and analysis of acinar cell granularity via transmission light microscopy (*right*) (n = 4). (*C*) Quantification and representative images of proliferating Ki67$^+$ cells in normal tissue of C57/B6 mice after 86 weeks of nicotine treatment (n $\geq$ 3). (*D*) Fold change in *Sox9* mRNA expression levels in the pancreas of mice after 2 or 86 weeks of treatment compared with control levels (*dotted line*). (*E*) Quantification of SOX9$^+$ cells after exclusion of ductal cells, as well as transformed cells within neoplastic lesions (n = 4) (*left*). Representative images of SOX9$^+$ acinar cells (*right*). (*F*) Ex vivo colony formation after 2 weeks of in vivo nicotine treatment of Ela-KRAS$^{+/+}$ or Ela-KRAS^{G12V} mice. A representative image of quantified epithelial clones (*arrowheads*), pancreatic stellate cells (PSC) (*left*), and quantification (*middle*) are provided (see also Supplementary Figure 2*E*). Colony formation on Matrigel after 2 weeks of in vivo nicotine treatment of α7-nAChR$^{+/+}$ or α7-nAChR1$^{-/-}$ mice (*right*) (n = 3).

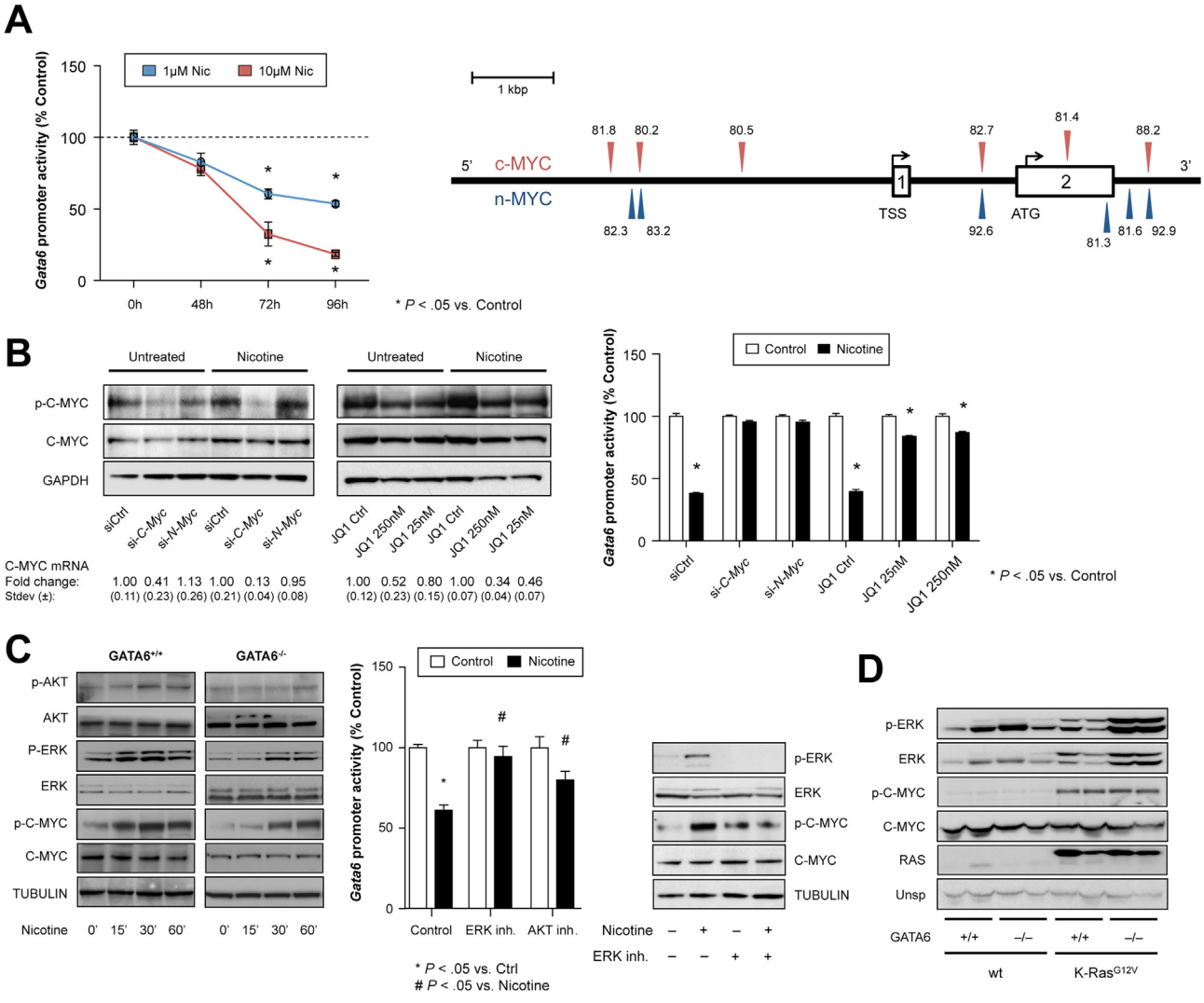
A
1μM Nic
10μM Nic
Gata6 promoter activity (% Control)
150
100
50
0
0h
48h
72h
96h
* P < .05 vs. Control
1 kbp
5'
c-MYC
n-MYC
3'
81.8
80.2
80.5
82.7
81.4
88.2
82.3
83.2
TSS
92.6
ATG
81.3
81.6
92.9
1
2
B
Untreated
Nicotine
Untreated
Nicotine
p-C-MYC
C-MYC
GAPDH
siCtrl
si-C-Myc
si-N-Myc
siCtrl
si-C-Myc
si-N-Myc
JQ1 Ctrl
JQ1 250nM
JQ1 25nM
JQ1 Ctrl
JQ1 250nM
JQ1 25nM
C-MYC mRNA
Fold change:
1.00 0.41 1.13 1.00 0.13 0.95
Stdev (±):
(0.11) (0.23) (0.26) (0.21) (0.04) (0.08)
1.00 0.52 0.80 1.00 0.34 0.46
(0.12) (0.23) (0.15) (0.07) (0.04) (0.07)
Control
Nicotine
Gata6 promoter activity (% Control)
150
100
50
0
siCtrl
si-C-Myc
si-N-Myc
JQ1 Ctrl
JQ1 25nM
JQ1 250nM
* P < .05 vs. Control
C
GATA6+/+
GATA6-/-
p-AKT
AKT
P-ERK
ERK
p-C-MYC
C-MYC
TUBULIN
Nicotine 0' 15' 30' 60' 0' 15' 30' 60'
Control
Nicotine
Gata6 promoter activity (% Control)
150
100
50
0
Control
ERK inh.
AKT inh.
* P < .05 vs. Ctrl
# P < .05 vs. Nicotine
p-ERK
ERK
p-C-MYC
C-MYC
TUBULIN
Nicotine – + – +
ERK inh. – – + +
D
p-ERK
ERK
p-C-MYC
C-MYC
RAS
Unsp
GATA6 +/+ –/– +/+ –/–
wt
K-RasG12V
E
Murine acinar cells
Gata6+/+ K-Ras+/+
Gata6 –/– K-Ras+/+
Gata6+/+ K-RasG12V
Gata6 –/– K-RasG12V
RAS-GTP
Total RAS
GATA6
Ctrl Nic TGFa Ctrl Nic TGFa Ctrl Nic TGFa Ctrl Nic TGFa
K-RasG12V-CEU
Endogenous Ras
Human PDAC
BXPC3 K-Ras+/+
PDAC-215 K-RasG12D
PDAC-253 K-RasG12D
RAS-GTP
Total RAS
ß-ACTIN
Ctrl Nic Ctrl Nic Ctrl Nic
Control
Nicotine
Fold increase in proliferation
50
40
30
20
10
0
Gata6 +/+ –/– +/+ –/–
WT
K-RasG12V
* P < .05 vs. Control
F
Gata6 +/+
Gata6 –/–
Tumor weight (mg)
200
150
100
50
0
Control
Nicotine
10^6 10^6 10^5 10^6 10^6 10^5
WT
K-RasG12V
WT
K-RasG12V
* P < .05 vs. Control
Gata6+/+ K-Ras+/+
Gata6 –/– K-Ras+/+
Control
Nicotine
10^6 cells
10^5 cells
Gata+/+;KrasG12V
GATA6–/–;KrasG12V

up-regulation of genes associated with a pancreatic stem cell signature after treatment with nicotine or with cigarette smoke extract (Figure 4*A* and Supplementary Figure 4*A*) in fully transformed pancreatic cancer cells. Colony formation and sphere formation over several passages were also significantly enhanced in response to nicotine treatment (Figure 4*B*), further corroborating a nicotine-mediated promotion of cancer stem cells (CSCs). Importantly, enhanced sphere formation could be abrogated by inhibiting nicotine binding to its receptor using the pan-nAChR inhibitor mecamylamine, the α7-nAChR inhibitor bungarotoxin or by inhibiting ERK or AKT signaling (Figure 4*C* and Supplementary Figure 4*B*). Lastly, in vivo tumorigenicity was also significantly higher in nicotine-treated murine PDAC cells, resulting in an increased CSC frequency (Figure 4*D*).

In addition, it has been shown that moderate levels of reactive oxygen species (ROS) have an important role in regulating self-renewal of CSCs, which could represent another putative mechanism of action for nicotine in the pancreas.[22] Previous studies demonstrated up-regulation of reduced nicotinamide adenine dinucleotide phosphate oxidase (*Nox*) in a *K-Ras*—dependent fashion, as well as in the context of *Mist1*-deficiency.[15] Consistently, in primary cancer cells, we observed *Nox1* up-regulation (Supplementary Figure 5*A*, *left*) and increased ROS levels (Supplementary Figure 5*A*, *middle/right*), most prominently in anchorage-independent and stem cell-enriching sphere cultures. In addition, nicotine strongly increased ROS production in C57/B6 acinar colonies, which was completely reversed by the NOX1 inhibitor STK30183 or the antioxidant n-acetyl-cysteine (Supplementary Figure 5*B*). This effect of nicotine was transient in C57/B6 colonies, but persisted in colonies derived from *K-Ras*$^{+/\text{LSL-G12D}}$;*Pdx-1*-Cre mice. In addition, in primary cancer cells, the increase in ROS levels was abrogated by co-treatment with STK30183 or n-acetyl-cysteine, or mecamylamine (Supplementary Figure 5*C*). Co-treatment with STK301831 or n-acetyl-cysteine also attenuated the nicotine-induced *Gata6* promoter repression (Supplementary Figure 5*D*), which supports our hypothesis for a putative mechanistic link between ROS, nicotine, and *Gata6* signaling.

Because our studies in nontransformed primary murine acinar cells highlighted *Gata6* as a key player in both nicotine-mediated acinar de-differentiation and K-RAS activation, we stably infected murine PDAC cells with a *Gata6*-expressing lentivirus and observed that overexpression of *Gata6* resulted in morphologic and cellular changes consistent with a more epithelial-like cellular phenotype, including down-regulation of stemness-related genes (Supplementary Figures 4*C* and *D* and 5*A*). More importantly, *Gata6* overexpression rendered murine PDAC cells completely refractory to the potentiating effects of nicotine in all in vitro assays tested (Figure 4*B* and *C*), and the ability of nicotine to enhance in vivo tumorigenicity was also abrogated in *Gata6*-overexpressing cells (Figure 4*E*), indicating that loss of *Gata6* is a necessary step for nicotine to promote cancer stem cell phenotypes, such as self-renewal and tumorigenicity.

Lastly, we analyzed expression of epithelial-mesenchymal transition (EMT)-related genes in murine PDAC cancer cells treated with nicotine or cigarette smoke extract. We observed a significant down-regulation of E-cadherin, and mesenchymal genes *Zeb1* and *Snai1* were strongly up-regulated (Figure 5*A* and Supplementary Figure 6*A*). Functionally, cell migration was significantly enhanced after nicotine treatment and was associated with an enhanced mesenchymal gene expression pattern (Figure 5*B*). Interestingly, nicotine-induced EMT gene expression could be reversed using mecamylamine, inhibitors of ERK and AKT or antioxidants (Figure 5*A* and *C* and Supplementary Figure 5*E*). To test these effects in vivo, we quantified the number of circulating pancreatic cells as a very sensitive readout for a metastatic phenotype in the blood stream of KPC mice. We observed a significant increase of circulating pancreatic cells (ie, red fluorescent protein—positive and epithelial cell adhesion molecule–positive cells) in nicotine-treated mice (Figure 5*D*). In addition, we used specific primers flanking the Lox-Stop-Lox cassette in the *K-Ras* gene to detect cells containing the recombined *K-Ras* allele in the liver by polymerase chain reaction (PCR) and subsequent nested PCR. This highly specific assay demonstrated an increased dissemination of pancreas-derived cells to the liver in nicotine-treated mice (Figure 5*E*). Sequencing of the PCR

Figure 3. Nicotine suppresses GATA6 via ERK/MYC activation. (*A*) *Gata6* promoter activity in murine acinar cells transfected with a *Gata6* promoter reporter vector and treated with 1 or 10 μM nicotine for the indicated times (*left*). In silico analysis of C-MYC binding sites (*red arrowheads*) and N-MYC binding sites (*blue arrowheads*) in the *Gata6* promoter (*right*). Numbers depict core similarity values. (*B*) Analysis of C-MYC and phospho-C-MYC protein and messenger RNA (mRNA) expression (*left*), and *Gata6* promoter activity (*right*) after silencing or chemical inhibition of C-MYC. mRNA levels are normalized to respective controls. (*C*) Western blot analysis of ERK/MYC pathway members after the indicated time of nicotine exposure in *Gata6*$^{+/+}$ vs *Gata6*$^{-/-}$ murine acinar cells (*left*). Measurement of *Gata6* promoter activity at 72 hours (*middle*) and protein expression of ERK/MYC pathway members 30 minutes after treatment with the indicated compounds (*right*). (*D*) Western blot analysis of key nicotine network members in *Gata6*$^{+/+}$or *Gata6*$^{-/-}$ murine acinar cells before and after the introduction of an activating *K-Ras*^{G12V} mutation. (*E*) RAS-GTP was determined in murine acinar cells with different *Gata6* and *K-Ras* statuses using transforming growth factor—α (TGFα) as a positive control (*left*). Ras-GTP in the human cell lines BXPC3, PDAC-215, and PDAC-253 after stimulation with nicotine for 6 days (*middle*). Proliferation in response to nicotine treatment in murine acinar cells with the indicated *Gata6* and *K-Ras* profile (*right*). (*F*) Tumor weight quantification (*left*) and representative tumor images (*right*) of Gata6-proficient or Gata6-deficient murine acinar cells expressing wt or mutant K-Ras and treated as indicated. ($n \geq 3$ for all experiments, $n \geq 2$ for Western blot.)

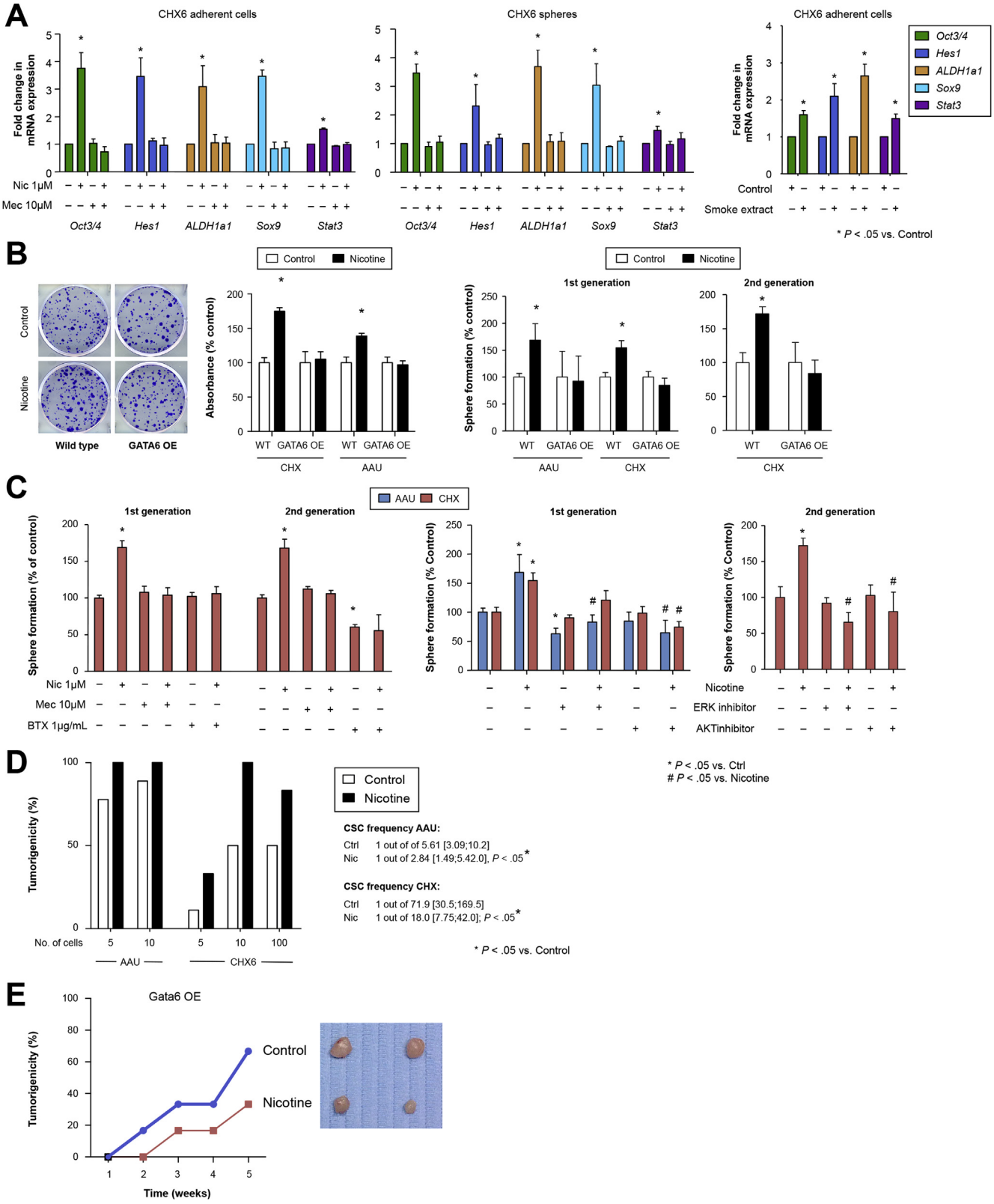

Figure 4. Nicotine promotes a cancer stem cell phenotype. (*A*) messenger RNA (mRNA) expression levels of stemness genes in adherent (*left*) and sphere cultures (*middle*) of murine PDAC cells treated as indicated (see also Supplementary Figure 4*A*), or with cigarette smoke extract (*right*) (n = 2). Data are normalized to control levels. (*B*) Colony formation (*left*) and serial sphere formation (*right*) of wt or *Gata6*-overxpressing murine PDAC cells. (*C*) Sphere formation and serial passaging of murine PDAC cells after 6 days of pretreatment with the indicated compounds. (*D*) Tumorigenicity limiting dilution assays for murine PDAC cells after 6 days of nicotine pretreatment. CSC frequencies were calculated using ELDA software; mean [95% confidence interval]. (*E*) Tumorigenicity experiments of wt or *Gata6* overexpressing murine PDAC cells after 6 days of nicotine pretreatment. (n ≥ 3 for all experiments.)

products confirmed a recombined single Lox sequence (Supplementary Figure 6C).

Considering the role of *Gata6* in inhibiting CSC properties demonstrated here, we next measured whether the overexpression of *Gata6* could similarly influence EMT and metastasis. *Gata6*-overexpressing murine PDAC cells had a more epithelial-like gene expression profile and a decreased in vitro migratory capacity compared with wt cells (Figure 5*F* and Supplementary Figure 6*B*). Interestingly, although nicotine could potentiate the migratory and metastatic capacity of unmodified murine PDAC cells in a wound healing and in vivo intrasplenic metastatic assay, nicotine had no metastasis-promoting effects on *Gata6* overexpressing cells in vivo (Figure 5*F*, *right*).

Metformin Prevents Pancreatic De-Differentiation and Carcinogenesis

Metformin may reduce the risk for developing pancreatic cancer[23] and may inhibit several of the mechanisms found necessary for the effects of nicotine.[24] Nicotine-induced effects in vitro and in vivo could be offset by co-treatment with metformin (Figure 6*A* and Supplementary 1*A*), which is shuttled into cells by organic cation transporters (Supplementary Figure 7*A*). Specifically, although metformin had no impact on the incidence of low-grade PanINs, we observed significantly fewer high-grade PanINs and no PDAC lesions (Figure 6*A*) in mice treated with nicotine and metformin. Of note, metformin also prevented PDAC development in the absence of nicotine, and most strikingly, we detected no micrometastases (0 of 9 mice) in mice treated with nicotine and metformin. At the same time, metformin treatment had no impact on the body weight or food intake of treated mice (Supplementary Figure 7*B*).

Mechanistically, metformin induced expression of *Gata6* and *Mist1* and promoted an acinar cell re-differentiation program, as demonstrated by an enhanced acinar gene signature (Figure 6*B*). Although nicotine treatment alone had the opposite effect, the combination of nicotine and metformin resulted in markedly higher expression of acinar genes compared with control or nicotine-treated mice. In addition, metformin treatment attenuated the nicotine-induced stem cell signature in wt pancreata as well as in primary PDAC cells (Figure 6*B* and Supplementary Figure 7*C*). Because loss of *Gata6* activity is necessary for nicotine's cancer-promoting effects, we measured *Gata6* promoter activity in the presence of metformin. Co-administration of metformin, together with nicotine, resulted not only in higher *Gata6* promoter activity, but also in increased GATA6 protein levels (Figure 6*C*) and inhibition of C-MYC. Similar effects were observed when ERK was inhibited, suggesting that the key players of the nicotine-induced pro-tumor effects are efficiently silenced by metformin (Figure 6*C* and Supplementary Figure 7*D*). In addition, and probably related to inhibition of MYC phosphorylation, metformin was able to revert nicotine-induced proliferation, which was more striking in *Gata6*-deficient/*K-Ras*^{G12V} cells (Figure 6*D*).

Finally, metformin also had strong effects on transformed PDAC cells (Figure 6*E* and Supplementary Figure 7*E*), suggesting that metformin not only promotes acinar differentiation and inhibits the progenitor phenotype induced by nicotine, but also has a direct inhibitory effect on pancreatic cancer (stem) cells. Interestingly, we also found that enhanced ROS production after nicotine treatment was reduced to control levels in acinar colonies generated from *K-Ras*$^{+/LSL\text{-}G12D}$;*Pdx-1*-Cre mice and in primary PDAC cells after metformin treatment (Supplementary Figure 7*F*). Because both nicotine and metformin induce adenosine monophosphate–activated protein kinase (AMPK) phosphorylation (Supplementary Figure 7*G*), the observed effects were likely independent of AMPK as metformin's primary mechanism of action.

Discussion

Proper acinar differentiation is an important attribute of pancreatic tissue homeostasis. Loss of acinar differentiation, for example, by knockout of *Gata6*, results in increased acinar apoptosis and proliferation, acinar-to-ductal metaplasia, and adipocyte transdifferentiation.[14] Here we show for the first time that a similar, albeit subtler phenotype is induced by nicotine using concentrations regularly found in smokers. Eventually, these changes, if they occur in the context of mutant *K-Ras* result in substantial acceleration of PDAC development.

In line with the observation that many aged individuals carrying *K-Ras* mutations are perfectly healthy, mice carrying *K-Ras* mutations very rarely develop PDAC. However, cells harboring *K-Ras* oncogenes will eventually progress to PanIN and PDAC if exposed to chronic injury (eg, chronic pancreatitis),[7] which contributes to tumor progression by surmounting the senescence barrier characteristic of low-grade PanINs. Here we identified nicotine as a potent initiator of the oncogenic transformation of murine pancreatic cells bearing activating *K-Ras* mutations. Importantly, nicotine-treated mice did not exhibit signs of acute or chronic pancreatitis as evidenced by normal serum pancreatic enzyme levels and unperturbed pancreatic histology, excluding that the effects induced by nicotine are due to inflammation. Rather, we found that nicotine altered pancreatic tissue homeostasis by inducing acinar cell de-differentiation and enhancing pancreatic progenitor cell activity, the effects of which were mediated by α7-nAChR. However, we do not formally exclude that nicotine might also be affecting the nonacinar compartment (immune cells and stellate cells) either directly or secondarily due to enhanced acinar-to-ductal metaplasia. Although wt animals did not show any inflammatory response to nicotine exposure, we did observe increased infiltration of macrophages in the nicotine-treated Kras mice, suggesting a secondary pro-tumorigenic effect mediated by M2-polarized macrophages. Therefore, nicotine is likely also affecting cell types other than the acinar compartment of the pancreas.

Using primary acinar cell cultures, we were able to dissect nicotine's mechanism of action ex vivo. Specifically, we show that nicotine strongly activates AKT, ERK-1/2, and

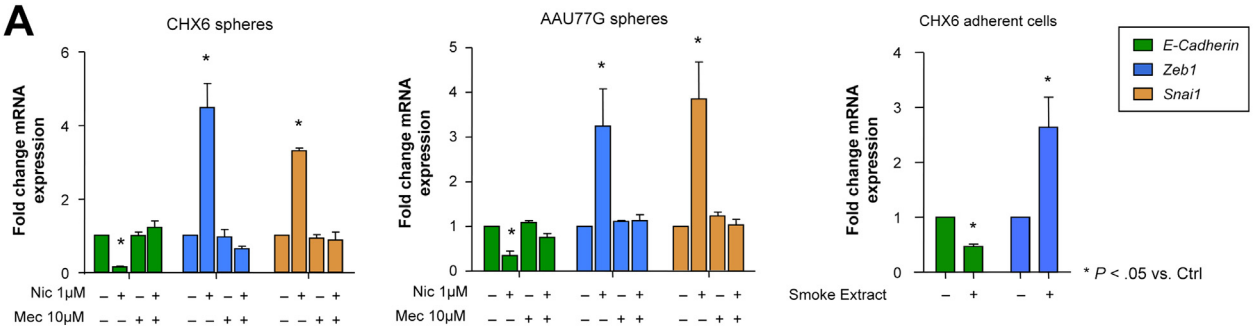
A
CHX6 spheres
AAU77G spheres
CHX6 adherent cells
Fold change mRNA expression
E-Cadherin
Zeb1
Snai1
Nic 1μM
Mec 10μM
Smoke Extract
* P < .05 vs. Ctrl

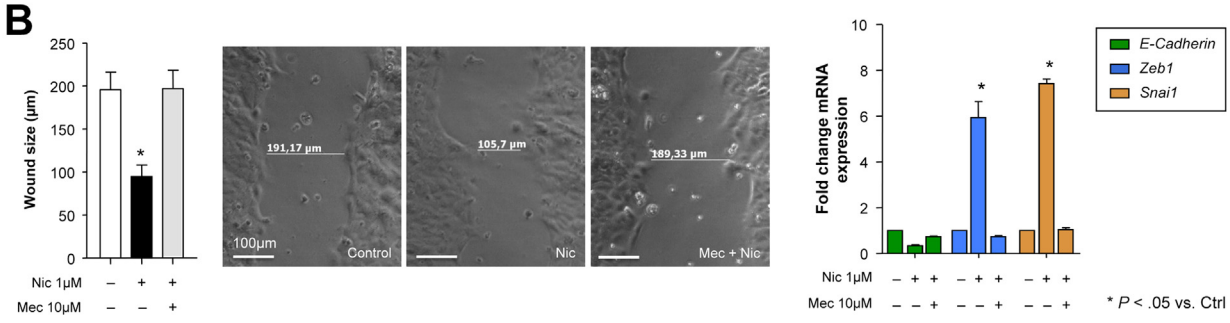
B
Wound size (μm)
191,17 μm
105,7 μm
189,33 μm
100μm
Control
Nic
Mec + Nic
Fold change mRNA expression
E-Cadherin
Zeb1
Snai1
Nic 1μM
Mec 10μM
* P < .05 vs. Ctrl

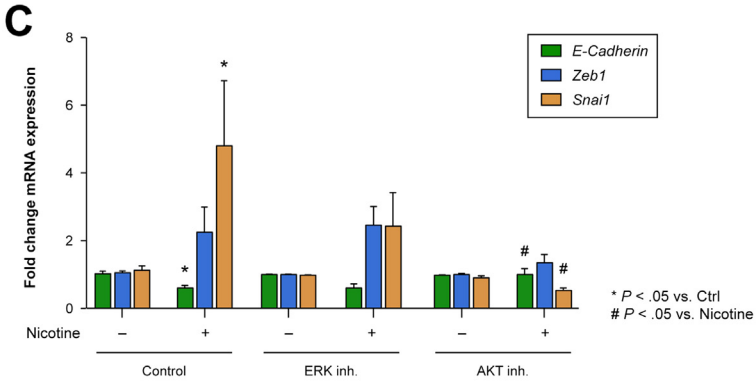
C
Fold change mRNA expression
E-Cadherin
Zeb1
Snai1
Nicotine
Control
ERK inh.
AKT inh.
* P < .05 vs. Ctrl
# P < .05 vs. Nicotine

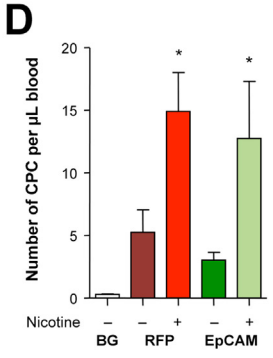
D
Number of CPC per μL blood
Nicotine
BG
RFP
EpCAM

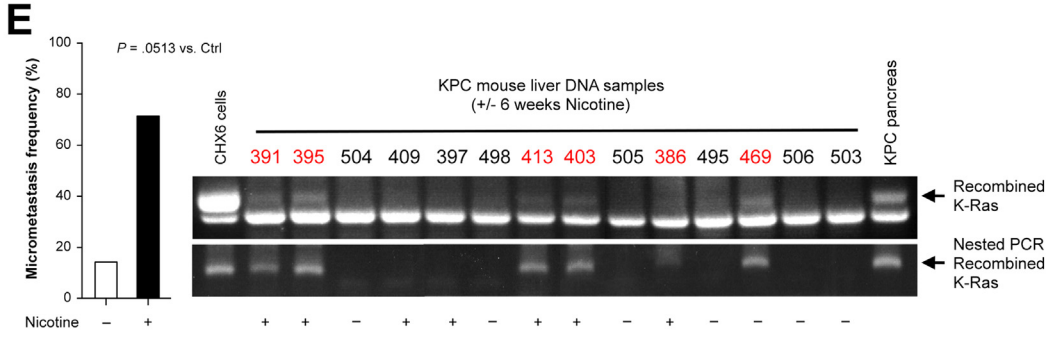
E
P = .0513 vs. Ctrl
Micrometastasis frequency (%)
Nicotine
KPC mouse liver DNA samples
(+/- 6 weeks Nicotine)
CHX6 cells
391 395 504 409 397 498 413 403 505 386 495 469 506 503
KPC pancreas
Recombined K-Ras
Nested PCR
Recombined K-Ras

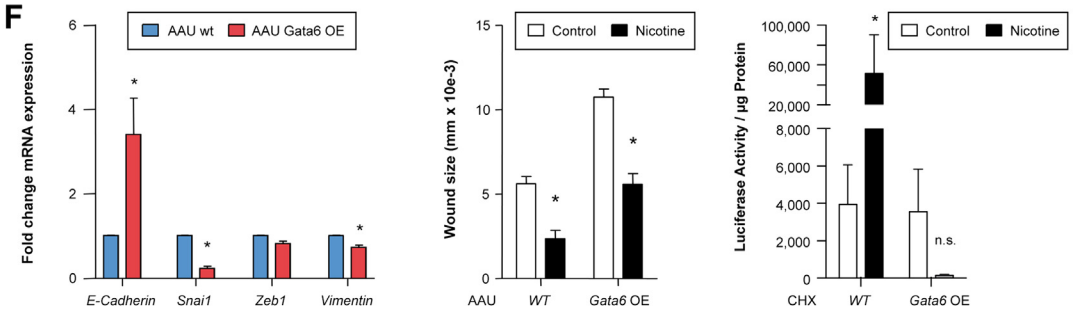
F
AAU wt
AAU Gata6 OE
Fold change mRNA expression
E-Cadherin
Snai1
Zeb1
Vimentin
Control
Nicotine
Wound size (mm x 10e-3)
AAU
WT
Gata6 OE
Luciferase Activity / μg Protein
n.s.
CHX

C-MYC, the latter of which has already been shown to directly inhibit the *Gata6* promoter.[21] Using a *Gata6* promoter reporter, we observed that nicotine treatment resulted in substantial suppression of *Gata6* promoter activity, which could be prevented by inhibition of either ERK1/2 or MYC (Figure 3*A*–*C*). Of note, silencing of both C-MYC and N-MYC prevented nicotine-mediated inhibition of *Gata6* promoter activity. This is not surprising, as N-MYC has been shown to be able to functionally replace C-MYC in mouse development, cell growth, and differentiation[25], and the *Gata6* promoter contains binding sites for both C-MYC and N-MYC (Figure 3*A*). Nicotine therefore directly suppresses the key acinar fate regulator *Gata6* and, subsequently, downstream players such as *Mist1*, resulting in loss of pancreatic acinar cell markers and increased cellular plasticity with subsequently enhanced progenitor activity (Figure 2). It appears reasonable to postulate that this nicotine-induced de-differentiation of the acinar compartment via suppression of *Gata6* renders the cells more susceptible to oncogenic transformation by *K-Ras* alone or in combination with mutant or lost Trp53.[26] In this context, it is important to note that nicotine also markedly enhanced RAS activity, which was previously linked to initiation of *K-Ras*–driven PDAC development,[27] but this activation was only apparent under specific circumstances: when *Gata6* levels were low and in the presence of activating *K-Ras* mutations, both of which can be fond in *K-Ras* mutant mice chronically treated with nicotine and fully transformed PDAC lesions.

Our findings therefore suggest a nicotine-induced chain of transforming events in the pancreas, which eventually culminate in the development of PDAC (Figure 7). First, nicotine activates AKT and ERK1/2 resulting in increased acinar cell proliferation and subsequent activation of the acinar compartment. Nicotine also strongly activates C-MYC, which is downstream of pERK1/2, resulting in *Gata6* promoter inhibition, *Gata6* messenger RNA reduction, GATA6 protein loss, *Mist1* messenger RNA reduction, and, subsequently, overall loss of acinar commitment and differentiation. With mutant *K-Ras* at the center stage of pancreatic carcinogenesis, as is the case here utilizing mouse models of PDAC and also in many aged individuals, after nicotine-mediated acinar de-differentiation via repression of GATA6, nicotine acquires new capabilities, such as hyper-activating mutant K-RAS, even more efficiently activating ERK1/2 and AKT, and promoting other (cancer) stem cell–related genes and phenotypes—the culmination of which results in a substantially more rapid progression to PDAC. Of note, these data are in line with recent observations that *Gata6* deficiency in mouse models of PDAC results acceleration of cancer development, suggesting a tumor suppressive function for *Gata6* (Martinelli P et al, unpublished data, 2014).

Importantly, nicotine not only affects early pancreatic carcinogenesis, but also promotes tumor progression at later stages. Nicotine enhanced the CSC compartment, as evidenced by up-regulation of stemness-associated genes, increased self-renewal capacity, and in vivo tumorigenicity. In addition, nicotine-mediated enhancement of CSC plasticity also translated into increased EMT and subsequently increased numbers of circulating pancreas-derived cells and liver (micro-)metastases; however we cannot rule out an additional contributing role of nicotine on the stroma. Importantly and in line with our initiation data, overexpression of *Gata6* alone in transformed murine PDAC cells did not revert the state of CSCs, but rendered these cells less aggressive and completely refractory to the stimulatory effects of nicotine. Although we cannot yet provide an explanation for why nicotine potently activates *K-Ras*–mutant cancer cells when GATA6 levels are low, we can only speculate that loss of GATA6 allows nicotine (in the context of mutant *K-Ras*) to more efficiently activate pathways like mitogen-activated protein kinases (eg, ERK1/2) and K-RAS, perhaps via enhancement of upstream intracellular factors and/or ectopic programs that may additionally become activated/modulated when *Gata6* is lost.

From a therapeutic perspective, we observed that metformin virtually abrogated all of these effects of nicotine and essentially blocked development of *K-Ras*–initiated PDAC. Metformin, a well-tolerated drug for therapy of type 2 diabetes, has already received much attention recently, as metformin treatment in diabetic patients has been associated with reduced incidence of solid tumors, particularly pancreatic cancer.[28] However, to date, evidence supporting a direct anticancer effect for metformin had been missing. We found the protective effects of metformin on nicotine-induced pancreatic carcinogenesis to be independent of AMPK, although initially suggested as the primary mediator of metformin's effects.[29] More recently, however, a direct effect on the mitochondrial functionality has been described as the main mechanistic driver for its toxic action.[30] We have also recently shown that metformin irreversibly and

Figure 5. Nicotine promotes EMT and metastasis. (*A*) Messenger RNA (mRNA) expression levels of EMT genes in sphere cultures of murine PDAC cells treated as indicated. Results from adherent cultures are depicted in Supplementary Figure 6*A*. (*B*) Scratch wound assays of murine PDAC cells. Quantification (*left*), representative images (*middle*), and normalized mRNA expression levels of EMT-related genes (*right*). (*C*) mRNA expression levels of EMT genes in sphere cultures of murine PDAC cells treated as indicated. (*D*) Quantification of circulating red fluorescent protein (RFP)-positive (n = 4 each) or epithelial cell adhesion molecule–positive (n = 6 each) cells in the peripheral blood of KPC or KPC-RFP mice treated with nicotine for 2 weeks. BG, background. (*E*) Detection of micrometastases by PCR specific for recombined *K-Ras*, and nested PCR for further amplification. *Red mouse numbers* indicate mice with micrometastases, and *left panel* shows quantification according to treatment. CHX6 PDAC cells and KPC pancreas were used as control samples. (*F*) mRNA expression levels of EMT genes in wt or *Gata6*-overexpressing murine PDAC cells (*left*). In vitro wound healing (*middle*) and liver metastasis after intrasplenic cell injection as determined by luciferase measurement in liver homogenates (*right*) (n ≥ 3 for all experiments).

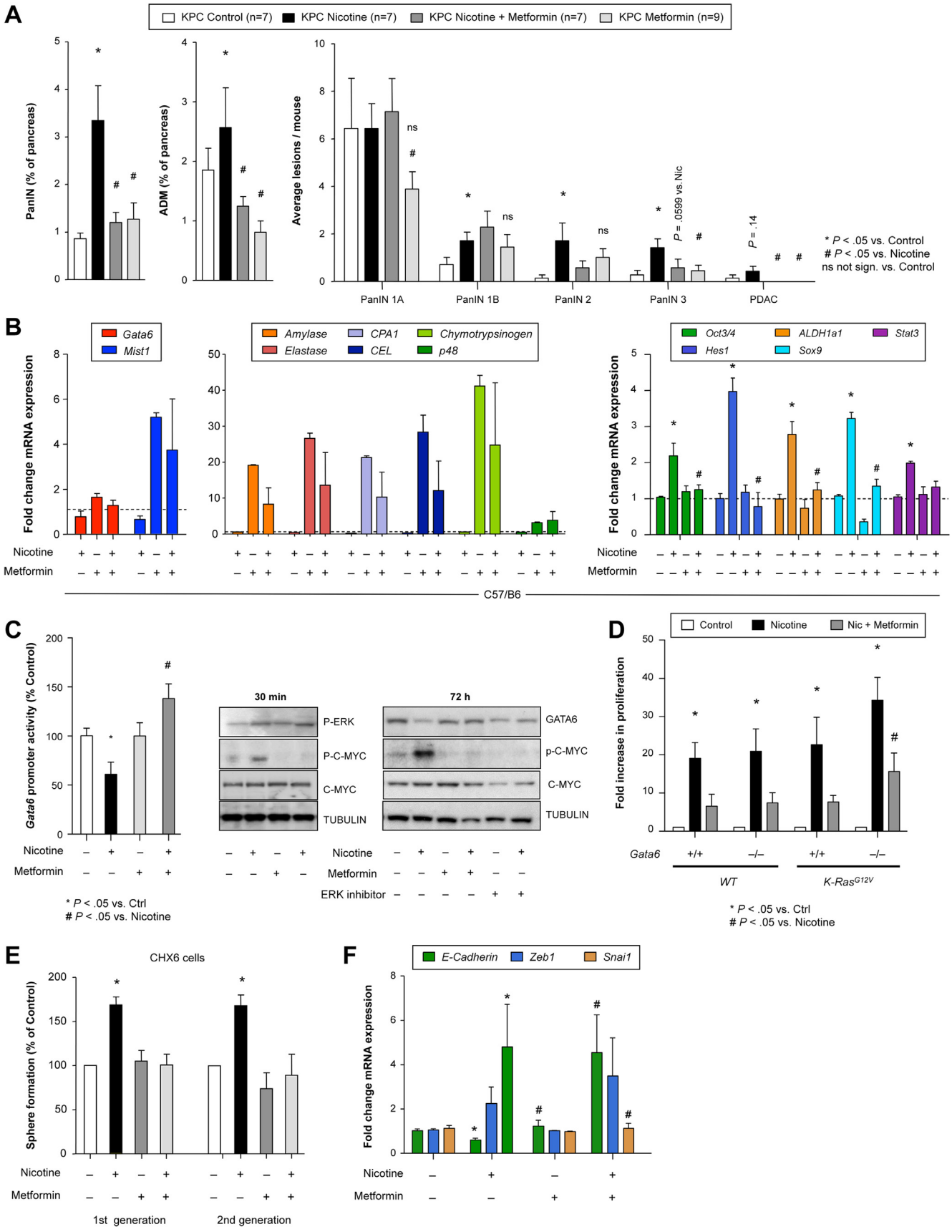

BASIC AND TRANSLATIONAL PANCREAS

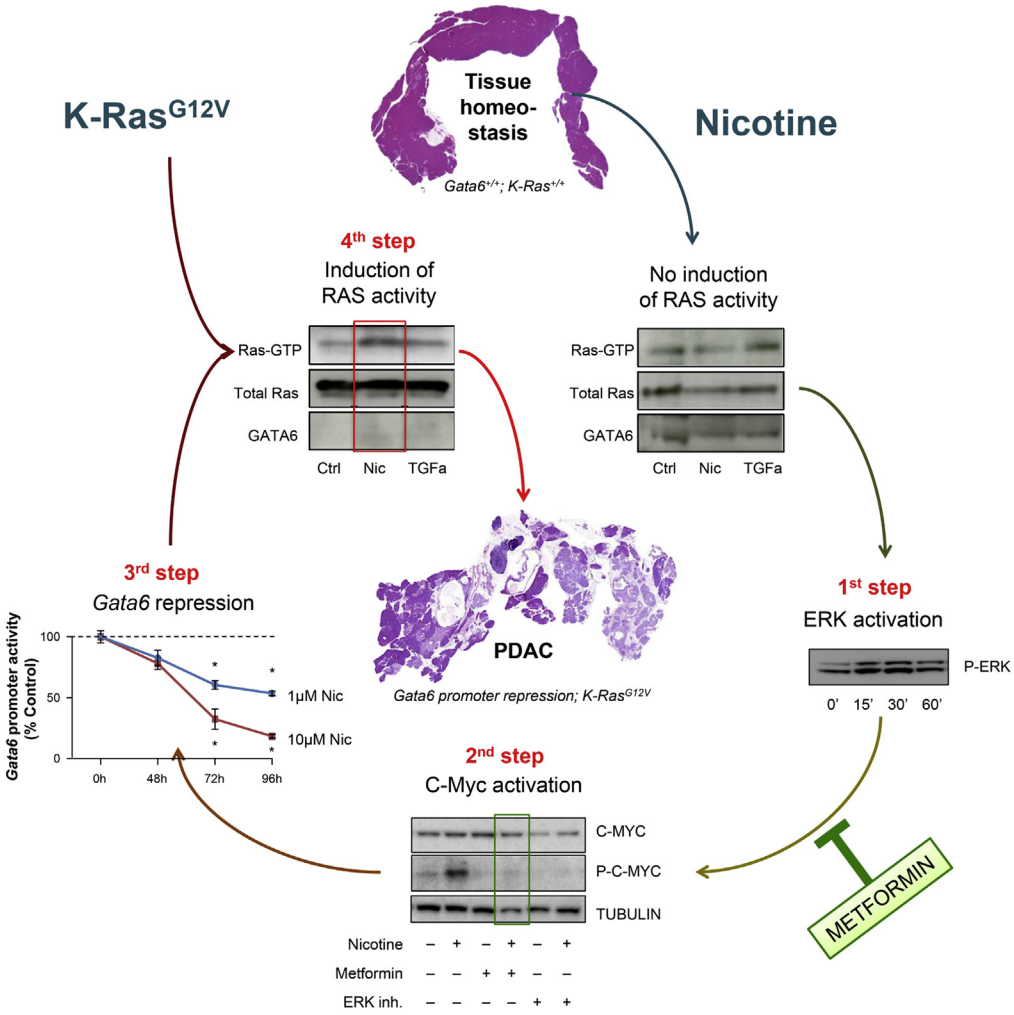

Figure 7. Summary of nicotine-induced chain of events in the pancreas.

independent of AMPK targets the CSC subpopulation by increasing ROS production in CSCs and reducing their mitochondrial transmembrane potential.[31] Metformin, however, has also been shown to reduce ROS production,[32] prevent Ca^{2+} influx,[33] and likely has many still undiscovered cellular effects/targets. We demonstrate that metformin abrogates nicotine-mediated *Gata6* down-regulation by inhibiting C-MYC activation. This results in the preservation and/or reinforcement of a committed acinar phenotype—an environment that is less prone to *K-Ras*—driven transformation and one in which nicotine can no longer exert its pro-tumorigenic effects, such as enhancement of CSC phenotypes, EMT genes, and proliferation in the context of fully transformed PDAC lesions. These effects can be rationalized by metformin's ability to inhibit C-MYC, as the latter represents a key pro-proliferative signal in cancer.[34] As expected, metformin's anti-cancer properties are likely multifactorial.

Figure 6. Metformin inhibits nicotine-induced progression of PDAC in KPC mice. For comprehensibility, results for Control and Nicotine from Figure 1*D* and *E* are displayed again in *panel A*. (*A*) Quantification of tissue area damaged by PanIN (*left*) or acinar-to-ductal metaplasia (ADM) + atrophy combined (*right*) in KPC mice treated with metformin and nicotine or metformin (*left*) and quantitative analysis of PanIN/PDAC frequency and grading (*right*). (*B*) Fold change in messenger RNA (mRNA) levels of the key acinar regulators (*left*), of acinar genes (*middle*), and of stem cell genes (*right*) in pancreatic tissue after 2 weeks of in vivo treatment with the indicated treatment combinations. Data are normalized to respective control levels (*dotted line*). (n = 2). For comprehensibility, results for Control and Nicotine from Figure 3 are displayed again in Figure 6*C*–*F*. (*C*) *Gata6* promoter activity after treatment as indicated (*left*), and protein quantification of members of the nicotine signaling network after 30 minutes (*middle*) or 72 hours (*right*). (*D*) Proliferation of *Gata6*$^{+/+}$ *or Gata6*$^{-/-}$ murine acinar cells expressing wt or mutant *K-Ras* and treated as indicated. (*E*) Sphere formation and serial passaging of murine PDAC cells after 6 days of pretreatment with the indicated compounds. (*F*) mRNA expression levels of EMT genes in murine PDAC cells after treatment with the indicated compounds. (n $\geq$ 3 for all experiments, n $\geq$ 2 for Western blot.)

Altogether, our results demonstrate that nicotine alone has strong effects on pancreatic cells during different stages of their "oncogenic development." Nicotine clearly paves the way for oncogenic transformation in normal tissue by inducing de-differentiation and cellular plasticity via down-regulation of *Gata6*, but also has pro-tumorigenic and pro-metastatic effects in fully transformed/*Gata6* low pancreatic cancer cells via promoting the cancer stem cell phenotype, including EMT. We show for the first time that by promoting acinar cell differentiation, treatment with metformin not only has a protective effect on the pancreas, but also counteracts the effects of environmental noxious substances via promotion of acinar commitment and differentiation. The findings reported in this study provide a strong rationale for eliminating nicotine intake as the main risk factor for PDAC and for designing new metformin-based treatment regimens for patients at high risk for developing PDAC.

Supplementary Material

Note: To access the supplementary material accompanying this article, visit the online version of *Gastroenterology* at www.gastrojournal.org, and at http://dx.doi.org/10.1053/j.gastro.2014.08.002.

References

1. Mack TM, Yu MC, Hanisch R, et al. Pancreas cancer and smoking, beverage consumption, and past medical history. J Natl Cancer Inst 1986;76:49–60.
2. Blackford A, Parmigiani G, Kensler TW, et al. Genetic mutations associated with cigarette smoking in pancreatic cancer. Cancer Res 2009;69:3681–3688.
3. Wu WK, Cho CH. The pharmacological actions of nicotine on the gastrointestinal tract. J Pharmacol Sci 2004; 94:348–358.
4. **Momi N, Ponnusamy MP**, Kaur S, et al. Nicotine/cigarette smoke promotes metastasis of pancreatic cancer through alpha7nAChR-mediated MUC4 upregulation. Oncogene 2013;32:1384–1395.
5. Dasgupta P, Rizwani W, Pillai S, et al. Nicotine induces cell proliferation, invasion and epithelial-mesenchymal transition in a variety of human cancer cell lines. Int J Cancer 2009;124:36–45.
6. Hingorani SR, Petricoin EF, Maitra A, et al. Preinvasive and invasive ductal pancreatic cancer and its early detection in the mouse. Cancer Cell 2003;4:437–450.
7. Guerra C, Schuhmacher AJ, Canamero M, et al. Chronic pancreatitis is essential for induction of pancreatic ductal adenocarcinoma by K-Ras oncogenes in adult mice. Cancer Cell 2007;11:291–302.
8. Lu X, Xu T, Qian J, et al. Detecting K-ras and p53 gene mutation from stool and pancreatic juice for diagnosis of early pancreatic cancer. Chin Med J (Engl) 2002; 115:1632–1636.
9. Howes N, Lerch MM, Greenhalf W, et al. Clinical and genetic characteristics of hereditary pancreatitis in Europe. Clin Gastroenterol Hepatol 2004;2:252–261.
10. Hingorani SR, Wang L, Multani AS, et al. Trp53R172H and KrasG12D cooperate to promote chromosomal instability and widely metastatic pancreatic ductal adenocarcinoma in mice. Cancer Cell 2005;7:469–483.
11. Pinho AV, Rooman I, Real FX. p53-dependent regulation of growth, epithelial-mesenchymal transition and stemness in normal pancreatic epithelial cells. Cell Cycle 2011; 10:1312–1321.
12. Kawaguchi Y, Cooper B, Gannon M, et al. The role of the transcriptional regulator Ptf1a in converting intestinal to pancreatic progenitors. Nat Genet 2002;32:128–134.
13. Sparks JA, Pauly JR. Effects of continuous oral nicotine administration on brain nicotinic receptors and responsiveness to nicotine in C57Bl/6 mice. Psychopharmacology (Berl) 1999;141:145–153.
14. Martinelli P, Canamero M, Del Pozo N, et al. Gata6 is required for complete acinar differentiation and maintenance of the exocrine pancreas in adult mice. Gut 2013; 62:1481–1488.
15. Direnzo D, Hess DA, Damsz B, et al. Induced Mist1 expression promotes remodeling of mouse pancreatic acinar cells. Gastroenterology 2012;143:469–480.
16. Rooman I, Real FX. Pancreatic ductal adenocarcinoma and acinar cells: a matter of differentiation and development? Gut 2012;61:449–458.
17. Zhu L, Shi G, Schmidt CM, et al. Acinar cells contribute to the molecular heterogeneity of pancreatic intraepithelial neoplasia. Am J Pathol 2007;171:263–273.
18. Rovira M, Scott SG, Liss AS, et al. Isolation and characterization of centroacinar/terminal ductal progenitor cells in adult mouse pancreas. Proc Natl Acad Sci U S A 2010;107:75–80.
19. **Kopp JL, Dubois CL**, Schaffer AE, et al. Sox9+ ductal cells are multipotent progenitors throughout development but do not produce new endocrine cells in the normal or injured adult pancreas. Development 2011;138:653–665.
20. McGehee DS, Role LW. Physiological diversity of nicotinic acetylcholine receptors expressed by vertebrate neurons. Annu Rev Physiol 1995;57:521–546.
21. Smith KN, Singh AM, Dalton S. Myc represses primitive endoderm differentiation in pluripotent stem cells. Cell Stem Cell 2010;7:343–354.
22. Shi X, Zhang Y, Zheng J, et al. Reactive oxygen species in cancer stem cells. Antioxid Redox Signal 2012; 16:1215–1228.
23. Evans JM, Donnelly LA, Emslie-Smith AM, et al. Metformin and reduced risk of cancer in diabetic patients. BMJ 2005;330:1304–1305.
24. Pierotti MA, Berrino F, Gariboldi M, et al. Targeting metabolism for cancer treatment and prevention: metformin, an old drug with multi-faceted effects. Oncogene 2013;32:1475–1487.
25. Malynn BA, de Alboran IM, O'Hagan RC, et al. N-myc can functionally replace c-myc in murine development, cellular growth, and differentiation. Genes Dev 2000;14: 1390–1399.
26. Kopp JL, von Figura G, Mayes E, et al. Identification of Sox9-dependent acinar-to-ductal reprogramming as the principal mechanism for initiation of pancreatic ductal adenocarcinoma. Cancer Cell 2012;22:737–750.
27. Daniluk J, Liu Y, Deng D, et al. An NF-kappaB pathway-mediated positive feedback loop amplifies Ras activity to

pathological levels in mice. J Clin Invest 2012; 122:1519–1528.

28. **Del Barco S, Vazquez-Martin A**, Cufi S, et al. Metformin: multi-faceted protection against cancer. Oncotarget 2011;2:896–917.
29. Shaw RJ, Bardeesy N, Manning BD, et al. The LKB1 tumor suppressor negatively regulates mTOR signaling. Cancer Cell 2004;6:91–99.
30. Scotland S, Saland E, Skuli N, et al. Mitochondrial energetic and AKT status mediate metabolic effects and apoptosis of metformin in human leukemic cells. Leukemia 2013;27:2129–2138.
31. **Lonardo E, Cioffi M**, Sancho P, et al. Metformin targets the metabolic achilles heel of human pancreatic cancer stem cells. PLoS One 2013;8:e76518.
32. Hou X, Song J, Li XN, et al. Metformin reduces intracellular reactive oxygen species levels by upregulating expression of the antioxidant thioredoxin via the AMPK-FOXO3 pathway. Biochem Biophys Res Commun 2010; 396:199–205.
33. Kisfalvi K, Eibl G, Sinnett-Smith J, et al. Metformin disrupts crosstalk between G protein-coupled receptor and insulin receptor signaling systems and inhibits pancreatic cancer growth. Cancer Res 2009;69:6539–6545.
34. Soucek L, Whitfield JR, Sodir NM, et al. Inhibition of Myc family proteins eradicates KRas-driven lung cancer in mice. Genes Dev 2013;27:504–513.

Author names in bold designate shared co-first authorship.

Received August 27, 2013. Accepted August 5, 2014.

Reprint requests
Address requests for reprints to: Bruno Sainz Jr, PhD, Spanish National Cancer Research Centre (CNIO), Madrid, Spain. e-mail: bruno.sainz@uam.es; fax: +34 91 497 53 53; or Christopher Heeschen, MD, PhD, Barts Cancer Institute, Centre for Stem Cells in Cancer & Ageing, London, UK. e-mail: c.heeschen@qmul.ac.uk; fax: +44 (0)20 7882 6110.

Acknowledgments
The authors are indebted to Flora Díaz Alcalá, Anaïs Moussy, and Jacob Insua Rodriguez for excellent technical assistance.

Conflicts of interest
The authors disclose no conflicts.

Funding
The research was supported by the ERC Advanced Investigator Grant (Pa-CSC 233460), European Community's Seventh Framework Programme (FP7/2007-2013) under grant agreement no. 256974 (EPC-TM) and the Subdirección General de Evaluación y Fomento de la Investigación, Fondo de Investigación Sanitaria (PS09/02129 & PI12/02643) and the Programa Nacional de Internacionalización de la I+D, Subprogramma: FCCI 2009 (PLE2009-0105; both Ministerio de Ciencia e Innovación, Spain), all to C.H.; and the Spanish Ministry of Economy and Competitiveness (SAF2011-30173 to M.B. and SAF2011-29530 to F.X.R.).

Supplementary Materials and Methods

In Vitro Treatment

Nicotine was added to cell cultures twice daily at a concentration of 1 μM (equivalent to the nicotine content in blood of smokers consuming one pack of cigarettes per day[1]). Cells were preincubated with all described inhibitors 1 hour before addition of nicotine: 10 μM mecamylamine (Sigma, St Louis, MO),[2] 1 μg/mL α-bungarotoxin (Sigma), 25 and 250 nM of the C-MYC inhibitor (+)-JQ1 (Selleck Chemicals, Houston, TX), 10 μM of the MEK inhibitor U0126 (Calbiochem, Billerica, MA), 10 μM of the AKT inhibitor LY294002, 3 mM metformin. Cigarette smoke extract containing approximately 1 μM nicotine was prepared by using commercial cigarettes with filters as described previously.[3] Silencer Select small interfering RNAs against *C-Myc* (5′-AGGUAGU GAUCCUCAAAAAtt-3′ and 5′-AGCUCACCUCUGAAAAGG Att-3′) or *N-Myc* (5′-GCAAGAACCCAGACCUCGAtt-3′ and 5′-AGAGCGCGCAGUGAACGAAtt-3′) were pooled, respectively, and transfected along with the *Gata6* promoter-LacZ-reporter vector into cells in suspension using Lipofectamine 2000 as per the manufacturer's instructions. A commercially available small interfering RNA negative control (Ambion, Life Technologies, Norwalk, CT) was included in all experiments for comparative purposes.

Sphere Formation Assay

Pancreatic cancer spheres were generated and expanded in DMEM-F12 (Invitrogen, Karlsruhe, Germany) supplemented with B-27 (Gibco, Karlsruhe, Germany) and basic fibroblast growth factor (PeproTech EC, London, UK). Five thousand cells/mL were seeded in ultra-low attachment plates (Corning B.V., Schiphol-Rijk, Netherlands). For serial passaging, 6-day-old spheres were harvested using 40-μm cell strainers, dissociated into single cells with trypsin, and then recultured for 5 additional days. Cultures were kept for no longer than 6 weeks after recovery from cryopreserved stocks (passage 3–4). Sphere formation was quantified using a Casy TTC cell counter (Roche Diagnostics, Barcelona, Spain). Counts $>$40 μm were considered spheres.

Colony-Formation Assay

Colony formation assays were performed as described previously.[4] Briefly, pancreata were collected upon necropsy and dissociated in 1 mg/mL Collagenase P (Roche, Rockford, IL) in Hank's balanced salt solution (Invitrogen, Carlsbad, CA) for 30 minutes at 37°C. After several rounds of washing and filtration, 3×10^4 viable cells/well were plated in a 24-well plate on semi-solid full Matrigel (BD, San Jose, CA). After 1 day, culture medium (DMEM-F12 supplemented with B-27 [Gibco, Grand Island, NY] and basic fibroblast growth factor [20 ng/mL; PeproTech, Rocky Hill, NJ]) was changed to serum-free RPMI 1640 medium containing 50 U/mL penicillin/streptomycin, and cells were incubated for 8 days. Colonies were fixed in 2% glutaraldehyde and counted after crystal violet staining (2%). For murine PDAC cell colony formation, 5000 wt or Gata6 overexpressing murine PDAC cells were plated in each well of a 6-well plate and treated twice a day for 7 days with a diluent control or 1 μM nicotine. Colonies were fixed and stained with 2% crystal violet in 70% EtOH, lysed in 10% sodium dodecyl sulfate and the absorbance value (A600) in each well was measured with a plate reader (ModulusII Plate Reader).

Scratch Wound Assay

Three scratch wounds were created in confluent cells using a p20 micropipette tip. Cells were washed twice with phosphate-buffered saline to remove cell debris, supplemented with assay medium, and monitored. Images were captured 24 hours after wounding. Three random wound sizes were measured per scratch.

DNA Constructs and Lentiviruses

The *Gata6* (8.8 kb/+2.0 kb) promoter-LacZ reporter vector (containing 8.8 kb of the 5′ *Gata6* flanking sequence, exon 1, intron 1, and part of the coding exon 2 linked upstream to the LacZ reporter) was kindly provided by Dr Ge-Hong Sun-Wada (Doshisha Women's College, Kyoto, Japan).[5] The $Kras^{G12V}$ coding sequence was excised from pBABEpuro-$Kras^{G12V}$ using BamHI and SalI and subsequently ligated into BamHI/XhoI-digested pRRL-CMV-IRES-Caerulean.[6] For the *Gata6* overexpressing vector pFG12-CMV-Gata6-GFP (kindly provided by Dr Clement Ho, University of Pennsylvania, Philadelphia, PA), the *Gata6* cds was PCR amplified from complementary DNA and subsequently cloned into the FG12-CMV-GFP lentivirus shuttle vector. Lentiviruses were produced as reported previously.[7] Briefly, viruses were generated by co-transfection of 293T cells with respective lentivirus shuttle backbone vectors (pRRL-CMV-$Kras^{G12V}$-IRES-Caerulean or pFG12-CMV-Gata6-GFP), the Pax2 packing plasmid and the vesicular stomatitis virus glycoprotein expression plasmid (pCMV-VSV-G) using standard $CaCl_2$ transfection protocols. Supernatants were collected 48 hours post-transfection, filtered through a 0.45 μm-pore-size filter (BD Biosciences), aliquoted, frozen, and subsequently titered on 293T cells by flow cytometry.

RNA Preparation and Reverse Transcription Polymerase Chain Reaction

Total RNA was isolated by the guanidine thiocyanate method using standard protocols. One microgram purified RNA was used for complementary DNA synthesis using the QuantiTect Reverse Transcription Kit (Qiagen, Barcelona, Spain), followed by SYBR green reverse transcription PCR using an Applied Biosystems 7500 real-time thermocycler (Applied Biosystems, Carlsbad, CA). Thermal cycling consisted of an initial 10-minute denaturation step at 95°C followed by 40 cycles of denaturation (15 seconds at 95°C) and annealing/extension (1 minute at 60°C). Primers used are listed in Supplementary Table 1.

DNA Preparation and Polymerase Chain Reaction

For verification of Cre-mediated recombination, DNA was isolated from homogenized pancreata and livers using standard phenol-chloroform extraction. PCR was performed as described previously,[8] using primers flanking the Lox–Stop–Lox cassette. Wild type *K-Ras* (622 bp), recombined Lox-*K-Ras*^{G12D} (650 bp), and Lox-Stop-Lox-cassette (500 bp) amplicons were visualized by gel electrophoresis. For all samples, gel areas corresponding to 650 bp were excised, gel purified (QIAquick Gel Extraction Kit; Qiagen, Valencia, CA) and nested PCR was performed as described. PCR products were again visualized by gel electrophoresis and those samples positive for a band at 650 bp were determined to have contained cells with a recombined Lox-*K-Ras*^{G12D}.

Western Blot Analysis

Total protein extracts were obtained using 1× RIPA buffer (Sigma) supplemented with phosphatase and protease inhibitors. Lysates were incubated for 1 hour at 4°C, centrifuged at 13,000 rpm for 20 minutes at 4°C, and total protein concentration was measured using the BCA Protein Assay kit (Pierce, Rockford, IL) according to manufacturer's instructions. Twenty-five to 100 μg protein were resolved by sodium dodecyl sulfate polyacrylamide gel electrophoresis and transferred to polyvinylidene difluoride membranes. After antibody incubations, bound antibody complexes were detected by enhanced chemoluminiscence (Amersham, Little Chalfont, UK). A complete list of antibodies used is included in Supplementary Table 2.

Flow Cytometry

For cytometry, the following antibodies were used: anti–epithelial cellular adhesion molecule–allophycocyanin (BD) or appropriate isotype-matched control antibodies or an Aldefluor Kit (STEMCELL Technologies, Vancouver, BC, Canada) using 33 μM 4-diethylaminobenzaldehyde (inhibitor of ALDH) for ALDH+ cell gating. 4′,6-Diamidino-2-phenylindole (eBiosciences, San Diego, CA) was used to exclude dead cells. Samples were analyzed by flow cytometry using a FACS Canto II or an INFLUX cell sorter (BD), and data were analyzed with FlowJo software (Ashland, OR).

Cell Cycle Analysis

After trypsinization, cells were fixed in 70% ethanol and stored at −20°C. Before use, cells were centrifuged and pellets incubated in 10 μg/mL of RNase A for 1 hour at 37°C. Subsequently, cells were resuspended in 4′,6-diamidino-2-phenylindole solution (0.1% sodium citrate, 0.1% Triton X-100, and 1 μg/mL 4′,6-diamidino-2-phenylindole). Samples were analyzed by flow cytometry using a FACS Canto II (BD) and data were analyzed with FlowJo software.

Measurement of RAS Activity

RAS activity was determined by a RAF1 pull-down assay (Cell Biolabs, San Diego, CA) following the indicated time points of nicotine stimulation (approximately 30 minutes). Equal amounts of protein (3–5 mg) isolated from wt and Gata6$^{-/-}$ murine acinar cells (wt *K-Ras*), wt and Gata6$^{-/-}$ murine acinar cells stably expressing mutant *K-Ras*, BxPC3 (wt *K-Ras*), PDAC-215 (mutant *K-Ras*) and PDAC-253 (mutant *K-Ras*) were incubated with agarose beads coated with the RAS-binding domain of RAF1 to selectively isolate and pull down the active GTP-bound forms of RAS. Subsequently, precipitated GTP-RAS and total unprecipitated RAS (50 μg) were detected by Western blot analysis using anti–pan-RAS. Dilutions of the antibodies are listed in Supplementary Table 2.

Measurement of Intracellular Reactive Oxygen Species

The oxidation-sensitive fluorescent probe 2′,7′-dichlorodihydrofluorescein diacetate (H_2DCFDA) (Invitrogen) was used to analyze the total intracellular content of ROS. After treatment, cells were incubated with 2.5 μM H_2DCFDA (30 minutes, 37°C) and fluorescence was determined by flow cytometry.

Gata6 *Promoter* β-Galactosidase Activity Assay

Murine acinar cells were seeded at a density of 8×10^5 cells/well in 6-well plates. The following day, cells were transfected with 4 μg Gata6 promoter-LacZ-reporter vector using 1× linear polyethylenimine (Polysciences, Warrington, PA) as per the manufacturer's instructions. Cells were treated with the indicated treatments, and at the indicated times cultures were lysed in 1× RIPA buffer. To determine β-galactosidase levels, 40 μL undiluted lysates were incubated with 160 μL of 0.5 mM chlorophenol red-β-D-galactopyranoside diluted in 60 mM K_2HPO_4-KH_2PO_4 buffer (pH 8.0) containing 1.2 mM $MgCl_2$ in a 96-well plate for 24–48 hours at room temperature. Absorbance value (A570) in each well was measured with a plate reader (ModulusII Plate Reader; Promega, Madison, WI). Total protein concentrations were determined using a BCA protein assay kit (Pierce) and used to normalize β-galactosidase levels across all samples.

Identification of C-MYC Binding Sites

We performed in silico prediction of putative C-MYC binding sites in the *Gata6* gene on chromosome 18, and analyzed a total of approximately 9000 base pairs (approximately 4.3 kb upstream and 3.7 kb downstream of the transcription start site), spanning a large portion of the promoter region as well as exons 1 and 2. Using TFSEARCH software, we identified 6 putative C-MYC and N-MYC binding sites with high core and matrix similarity scores within this region of the *Gata6* gene.

In Vivo Treatment of Genetically Engineered Mice

Nicotine (Sigma) was administered at 100 μg/mL ad libitum via the drinking water supplemented with 2% sucrose.[9] Successful nicotine intake was verified in urine obtained during necropsy, using an enzyme-linked immunosorbent assay kit for mouse/rat cotinine (Calbiotech, Spring Valley, CA). Metformin was administered identically, at a concentration of 1 mg/mL.

Enumeration of Circulating Pancreas-Derived Cells

After 2 weeks of nicotine treatment, blood was extracted from 12- to 14-week-old *K-Ras*$^{+/LSL\text{-}G12D}$;*Trp53*$^{+/LSLR172H}$;*LSL-tdRFP*;*Pdx-1-Cre* mice (KPC-RFP) expressing a red fluorescent reporter protein,[10] or regular KPC mice and lysed with PharmLyse buffer (BD) according to manufacturer's instructions. Cells were stained with anti-mouse epithelial cellular adhesion molecule–allophycocyanin (2 μL, BD) in PBS + 1% fetal bovine serum for 45 minutes, counterstained with 4′,6-diamidino-2-phenylindole, and analyzed on an INFLUX sorter (BD). Mouse pancreas (KPC-RFP or KPC, respectively) was used as positive controls for gating. To ensure equal sample sizes, counting beads (Countbright, Invitrogen) were added to the blood samples, and CTC numbers were calculated accordingly.

In Vivo Tumorigenicity

Tumorigenicity experiments were performed as reported previously.[11] Briefly, cells were treated for 7 days, twice daily, with the indicated compounds at the indicated concentrations. Attached cells were then trypsinized, counted, serially diluted, resuspended in 40 μL Matrigel, and then injected subcutaneously into 6- to 8-week-old athymic nude mice (Harlan Laboratories, Indianapolis, IN). Cancer stem cell frequencies were determined from limiting dilution assay tumor results using ELDA software (WEHI, Parkville Victoria, Australia).

In Vivo Metastasis Assay

NU-Foxn1nu nude mice (Charles Rivers, L'Arbresle, France) were injected intrasplenically with 5×10^4 RFP/firefly luciferase expressing PDAC cells. Three weeks post injection, livers were explanted and homogenized in a volume of 1× phosphate-buffered saline equal to 3 times the weight of the tissue and subsequently lysed with passive lysis buffer (Promega). After centrifugation at 9000*g* for 30 minutes at 4°C, the supernatant was collected and firefly luciferase activity was measured using a Luciferase Assay System, according to the manufacturer's instructions (Promega). Total protein concentrations were determined using a BCA protein assay kit (Pierce).

Histopathology and Immunohistochemistry

Specimens were fixed in 10% buffered formalin and embedded in paraffin. For histopathologic analysis, pancreata were serially sectioned (3 mm) and every 10th section was stained with H&E. Representative sections were chosen for the grading and enumeration of lesions and quantification of tissue damage. These analyses were performed by a pathologist with demonstrated expertise in mouse pancreatic pathology (M.C.). Remaining sections were used for immunohistochemical studies with the primary antibodies indicated in Supplementary Table 3. After incubation with the primary antibodies, positive cells were visualized using 3,3-diaminobenzidine tetrahydrochloride plus. Counterstaining was performed with hematoxylin. Histologic quantification of digitalized slides was performed using Pannoramic Viewer (3DHistech, Budapest, Hungary) and Axiovision software (Carl Zeiss, Jena, Germany).

Transmission Electron Microscopy

For transmission electron microscopy, pieces of pancreas no larger than 2 mm^3 were fixed by immersion in a mixture of 2% glutaraldehyde in 0.1M cacodylate buffer at pH 7.4. After post fixation in 1% osmium tetroxide and staining with 1% tannic acid and 1% uranyl acetate, tissue samples were dehydrated, embedded in Epon 812. Semi-thin sections (0.5 μm), counterstained with toluidine blue, and areas for further analysis were randomly selected. Thin sections were counterstained with lead citrate and examined using a EM10 electron microscope (Zeiss).

Statistical Analyses

Results for continuous variables are presented as means ± SEM unless stated otherwise. Treatment groups were compared with the Mann-Whitney U test. P values $<.05$ were considered statistically significant. Statistical analyses were performed using GraphPad Prism 5.0 (San Diego, CA).

Supplementary References

1. Dasgupta P, Rastogi S, Pillai S, et al. Nicotine induces cell proliferation by beta-arrestin-mediated activation of Src and Rb-Raf-1 pathways. J Clin Invest 2006;116:2208–2217.
2. Heeschen C, Weis M, Aicher A, et al. A novel angiogenic pathway mediated by non-neuronal nicotinic acetylcholine receptors. J Clin Invest 2002;110:527–536.
3. Oltmanns U, Chung KF, Walters M, et al. Cigarette smoke induces IL-8, but inhibits eotaxin and RANTES release from airway smooth muscle. Respir Res 2005;6:74.
4. Jin L, Feng T, Shih HP, et al. Colony-forming cells in the adult mouse pancreas are expandable in Matrigel and form endocrine/acinar colonies in laminin hydrogel. Proc Natl Acad Sci U S A 2013;110:3907–3912.
5. Sun-Wada GH, Kamei Y, Wada Y, et al. Regulatory elements directing gut expression of the GATA6 gene during mouse early development. J Biochem 2004;135:165–169.
6. Drosten M, Dhawahir A, Sum EY, et al. Genetic analysis of Ras signalling pathways in cell proliferation, migration and survival. EMBO J 2010;29:1091–1104.

7. Torres R, Garcia A, Paya M, et al. Non-integrative lentivirus drives high-frequency cre-mediated cassette exchange in human cells. PLoS One 2011; 6:e19794.
8. Jackson EL, Willis N, Mercer K, et al. Analysis of lung tumor initiation and progression using conditional expression of oncogenic K-ras. Genes Dev 2001; 15:3243–3248.
9. Sparks JA, Pauly JR. Effects of continuous oral nicotine administration on brain nicotinic receptors and responsiveness to nicotine in C57Bl/6 mice. Psychopharmacology (Berl) 1999;141:145–153.
10. Luche H, Weber O, Nageswara Rao T, et al. Faithful activation of an extra-bright red fluorescent protein in "knock-in" Cre-reporter mice ideally suited for lineage tracing studies. Eur J Immunol 2007;37:43–53.
11. Hermann PC, Huber SL, Herrler T, et al. Distinct populations of cancer stem cells determine tumor growth and metastatic activity in human pancreatic cancer. Cell Stem Cell 2007;1:313–323.